Int J Clin Exp Pathol 2017;10(5):4955-4968
www.ijcep.com /ISSN:1936-2625/IJCEP0050769

Original Article

IRAK1 and TRAF6, inversely modulated by antitumor miR-146a-5p, markedly promotes the progression of NSCLC

Yu Zhang[1*], Rong-Quan He[2*], Xiao Wang[3], You-Rong Chen[2], Mei-Wei Li[2], Xiu-Ling Zhang[1], Jie Ma[2], Gang Chen[1], Xiao-Hua Hu[2]

Departments of [1]Pathology, [2]Medical Oncology, First Affiliated Hospital of Guangxi Medical University, Nanning, Guangxi Zhuang Autonomous Region, P. R. China; [3]Department of Orthopedics, China-Japan Union Hospital of Jilin University, Changchun, P. R. China. [*]Equal contributors and co-first authors.

Received February 13, 2017; Accepted February 25, 2017; Epub May 1, 2017; Published May 15, 2017

Abstract: MiR-146a-5p was proved to play significant roles in both tumorigenesis and development of diverse neoplasms, including non-small cell lung cancer (NSCLC). In the current research, qRT-PCR and immunohistochemistry were applied to verify the correlation of miR-146a-5p and IL-1 receptor-associated kinase 1 (IRAK1) or TNF receptor-associated factor 6 (TRAF6) at the tissue level. Besides, colorimetric tetrazolium (MTS) assay, fluorimetric resorufin viability assay, Hoechst 33342/PI double staining assay and caspase-3/7 activity assay were performed to research the effect of miR-146a-5p and IRAK1 or TRAF6 on cell growth and apoptosis at the cellular level. Meanwhile, Western blot was applied to detect IRAK1 and TRAF6 protein expression in NSCLC cells. And dual-luciferase reporter assay was performed to demonstrate whether miR-146a-5p could directly target 3'-untranslated region (3'-UTR) of IRAK1 and TRAF6. In conclusion, we identify that miR-146a-5p could act as an underlying tumor suppressor in NSCLC. Also, miR-146a-5p could down-regulate the IRAK1 and TRAF6 expression, leading to inhibition of proliferation and increased apoptosis of NSCLC cells. The effect of miR-146a-5p and its targets on the proliferation and apoptosis of NSCLC cells could provide new information in the target therapy of NSCLC.

Keywords: MiR-146a-5p, IRAK1, TRAF6, NSCLC

Introduction

Lung cancer, one of the lethal malignancies, remains the first leading cause of cancer-related deaths all over the world [1-3]. Non-small cell lung cancer (NSCLC) accounts for ~80% of total newly diagnosed lung cancers with a poor 5-year survival rate [4-7]. In the past few decades, strategies for the treatment and diagnosis of NSCLC have been improved. However, the prognosis and survival rate of NSCLC are still dismal [8-10]. Hence, the identification of efficient molecular biomarkers, such as microRNAs (miRNAs), is of paramount significance to the early screening and diagnosis of lung cancer.

MiRNAs are small non-coding RNAs. The current researches propose that miRNAs play pivotal roles in diverse biological processes, such as apoptosis and proliferation [11-13]. Many reports demonstrate that miRNAs dysregulate in a number of neoplasms such as renal cell carcinoma, gastric cancer and lung cancer [9, 14, 15]. As reported, miRNAs can regulate gene expression via binding to the 3'-untranslated region (3'-UTR) of targets [6, 16, 17]. In fact, various abnormally expressed miRNAs have been confirmed in different human cancers, including NSCLC [18-20]. Typically, miR-133b has been documented to suppress cell growth, cell migratory capacity and invasive ability of NSCLC cells by targeting MMP9 [18], while miR-543 enhances the proliferation and invasion of NSCLC cells via targeting PTEN [19].

Previous studies have certified that miR-146a-5p plays significant roles in proliferation, invasion and cell cycle in lung cancer, esophageal squamous cell carcinoma and bladder cancer

[21-23]. As reported, the effects of miR-146a-5p are conflicting depending on the cancer type. For example, miR-146a-5p can execute tumor suppressive function in ovarian or lung cancer as reported [24, 25], whereas in melanoma and anaplastic thyroid cancer, miR-146a-5p acts as a tumor oncogene and contributes to the initiation and progression [26, 27]. Previously, our study found that the low expression of miR-146a-5p was related to distant metastasis and advanced clinical TNM stage in NSCLC ($P<0.05$). In functional experiments, miR-146a-5p can inhibit cell growth, induce cellular apoptosis via targeting epidermal growth factor receptor (EGFR) and nuclear factor kappa B (NF-κB) signaling in NSCLC cells [25]. Besides, according to the prediction by MIRDB (available online: http://www.mirdb.org/) and Targetscan (available online: http://www.targetscan.org/), miR-146a-5p can target IL-1 receptor-associated kinase 1 (IRAK1) and TNF receptor-associated factor 6 (TRAF6), which have been functionally confirmed in inflammation, cardiac dysfunction, hepatocellular carcinoma and oral carcinoma [28-31]. As reported, IRAK1 is the first member of IRAK family and a key downstream component of the TLR signaling [32]. The missing of TLRs contributes to cancer, allergy and immune abnormalities [33, 34]. IRAK1 also can suppress I Kappa B Kinase Alpha (IK-Ba), and activate NF-κB [35]. TRAF6 is an amplified gene and can play essential roles in inflammation and immunity [36, 37]. TRAF6 also can be involved in the inhibition of apoptosis and potential of growth via activating NF-κB signaling [37, 38]. In addition, the relationship between miR-146a-5p and IRAK1 and TRAF6 in NSCLC has not been elucidated. In this study, the expression and function of miR-146a-5p, IRAK1 and TRAF6 are investigated in NSCLC patient tissues and cell lines.

Materials and methods

Tissue samples

We collected tissues from 65 NSCLC patients, which contained 35 male and 30 female lung tissues. All of these NSCLC tissues were collected from the First Affiliated Hospital of Guangxi Medical University, P. R. China (from January 2010 to December 2012). All of these NSCLC samples were randomly collected after surgical resection or biopsy. The study protocol was approved by the Ethical Committee of the First Affiliated Hospital of Guangxi Medical University, and the informed consents were provided by the clinicians and patients. The age of these cases was ranged from 29-83 years. Among 65 NSCLC patients, 44 cases were with lymph node metastasis, 46 cases were with advanced TNM stage (III-IV), 32 cases were with vessel invasion, and 23 cases were with larger tumor size (>3 cm).

Cell culture and re-expression or inhibition of miR-146a-5p in NSCLC cells

The human NSCLC cell lines (A549 and H460) were obtained from the Type Culture Collection of the Chinese Academy of Sciences, Shanghai, China and cultured as reported [39, 40]. The IRAK1, TRAF6 and EGFR-specific monoclonal antibodies were provided by Santa Cruz Biotechnology, Inc, America. The two cell lines were cultured in Dulbecco's modified essential medium (DMEM) medium supplemented with 10% heat-inactivated fetal bovine serum (Invitrogen Corp, Grand Island, NY, USA) and penicillin was added to the cell culture following the recommended conditions. All of the NSCLC cells were incubated at 37°C under a humidified 5% CO_2 atmosphere.

NSCLC cells were seeded at a density of 2.5×10^4 cells/well into 24-well plates and cultured at 37°C with 5% CO_2 for 24 h. Cells were transfected with miR-146a-5p mimic, miRNA mimic negative control, miR-146a-5p inhibitor, or miRNA inhibitor negative control (Ambion, Life Technologies Europe B.V.) respectively with Lipofectamine™ 2000 (Cat. No. 11668-019, Invitrogen) based on the manufacturer's instructions. The cells were transfected daily with the miR-146a-5p mimic or miR-146a-5p inhibitor up to day 10 [41]. After 0, 5 and 10 days of transfection, the expression of miR-146a-5p was detected [42]. Furthermore, the sequences of IRAK1 siRNA, TRAF6 siRNA and EGFR siRNA were as follows: 5'-AAG UUG CCA UCC UCA GCC UCC-3' (IRAK1); 5 EGFR siRNA'-CCCAGUCACACAUGAGAAU-3' (TRAF6); 5'GCAAAGTGTGTAACGGAATAGGTAT-3' (EGFR). And EGFR siRNA was used as positive control. The siRNAs were transfected into NSCLC cells by the same method as above.

RNA extraction and qRT-PCR

qRT-PCR was as described previously [25, 43, 44]. Blocks of clinical FFPE tissues were sec-

Table 1. The relationship between miR-146a-5p and its targets in NSCLC

Targets expression		n	MiR-146a-5p relevant expression ($2^{-\Delta Cq}$)		
			Mean ± SD	*t*	*P*
IRAK1	Negative	37	5.04273±8.402539	3.403	0.002
	Positive	28	0.33421±0.422453		
TRAF6	Negative	31	5.95823±8.908474	3.514	0.001
	Positive	34	0.33041±0.406994		

tioned at a thickness of 5-20 μm. The tissues were dewaxed by ethanol and xylene. Then the total RNA was extracted from tumor sections using the RNeasy FFPE Kit (Qiagen, KJ Venlo, Netherlands) according to the kit instructions. The RNA isolated from each sample was used for complementary DNA synthesis through the TaqMan MicroRNA Reverse Transcription Kit (Cat. No. 4366596, Tideradar Beijing Technology co., Ltd.) based on manufacturer's protocol. In addition, qRT-PCRs were performed using a LightCycler 480 (Roche, Shanghai). Each PCR cycle included 95°C for 10 seconds, 60°C for 10 seconds and 72°C for 10 seconds [45-47]. The miRNA was normalized to its reference miR-191 (Applied Biosystems Cat. No. 4427975-000490) and miR-103 (Applied Biosystems Cat. No. 4427975-000439) as reported [42, 45-49]. In addition, the quantification of miRNA or mRNA expression was analyzed by Delta Delta Ct method [50, 51].

Evaluation of immunostaining

The expression of IRAK1 and TRAF6 was detected by immunohistochemistry. The IRAK1 and TRAF6 antibody were purchased from Santa Cruz Biotechnology, Inc. USA. The immunohistochemistry procedure was according to the manufacturer's protocol. The average percentage of positive cells was scored by 2 independent pathologists as follows: 0 (0%); 1 (1-25%); 2 (26-50%); 3 (51-75%); and 4 (76-100%). The staining intensity was evaluated as follows: 0 (negative); 1 (weak); 2 (moderate) and 3 (strong). The percentage and staining intensity score were multiplied as the final pathological scores. The positive staining results were confirmed when the scores ≥ 2 [52, 53].

Cell proliferation

Cell proliferation was detected using a colorimetric tetrazolium (MTS) assay (CellTiter 96 Aqueous One Solution Cell Proliferation Assay G3580, Promega, Madison, USA). A549 and H460 cells (10^4 cells/mL) were seeded into 96-well plates. The miRNA mimic, miRNA inhibitor and siRNAs were transfected daily for 0, 5 and 10 days. After that, 20 μl MTS agent was added and the 96-well plates were cultured at 37°C with 5% CO_2 for 2 hrs. The detailed procedure was as described previously [39, 54-56]. Absorbance at 490 nm was assessed by a microplate reader.

Cell viability

To further confirm the results of the MTS assay, fluorimetric detection of resorufin (CellTiter-Blue Cell Viability Assay, G8080, Promega, Madison, WI, USA) was applied to detect the cell viability referenced to the manufacturer instructions An FL600 fluorescence plate reader (Bio-Tek, Winooski, Vermont, USA) was used for fluorimetry (ex: 560 nm/em: 590 nm). Fluorescence data were achieved as the fluorescence of treated sample/mock control × 100 [39, 54-56].

Caspase-3/7 activity detection

Caspase-3/7 activity was detected instantly by a synthetic rhodamine labeled caspase-3/7 substrate (Apo-ONE® Homogeneous Caspase-3/7 Assay, G7790, Promega, Madison, WI, USA) after the measurement of cell viability according to the manufacturer instructions [39, 54-56]. After incubation for 60 min at room temperature, an FL600 fluorescence plate reader (Bio-Tek, Winooski, Vermont, USA) was utilized to detect the fluorescence of each well (Ex: 499 nm/em: 512 nm). Caspase-3/7 activity was obtained from fluorescence of treated sample/mock control × 100.

Assessment of cell apoptosis

The effects of miR-146a-5p mimic, miR-146a-5p inhibitor, IRAK1 siRNA, TRAF6 siRNA or EGFR siRNA on cell apoptosis and morphology were evaluated by Hoechst 33342 and PI (Sigma-Aldrich N.V.) double fluorescent chromatin staining. Briefly, after treatment with miR-146a-5p mimic, inhibitor or siRNA, cells were washed using ice-cold PBS and then cells were stained for 15 min with Hoechst 33342 (1 mg/ml) and PI (1 mg/ml). After that, cells were

Table 2. The relationship between miR-146a-5p and its targets in NSCLC

Parameter		n	IRAK1 expression		*t*	*p*	TRAF6 expression		*t*	*P*
			Negative	Positive			Negative	Positive		
MiR-146a-5p expression*	Low	33	7 (21.2%)	26 (78.8%)	-5.859	<0.001	2 (6.1%)	31 (93.9%)	-6.772	<0.001
	High	32	30 (93.8%)	2 (6.2%)			29 (90.6%)	3 (9.4%)		

*Lung cancer patients were divided into two groups based on the median level of miR-146a-5p expression.

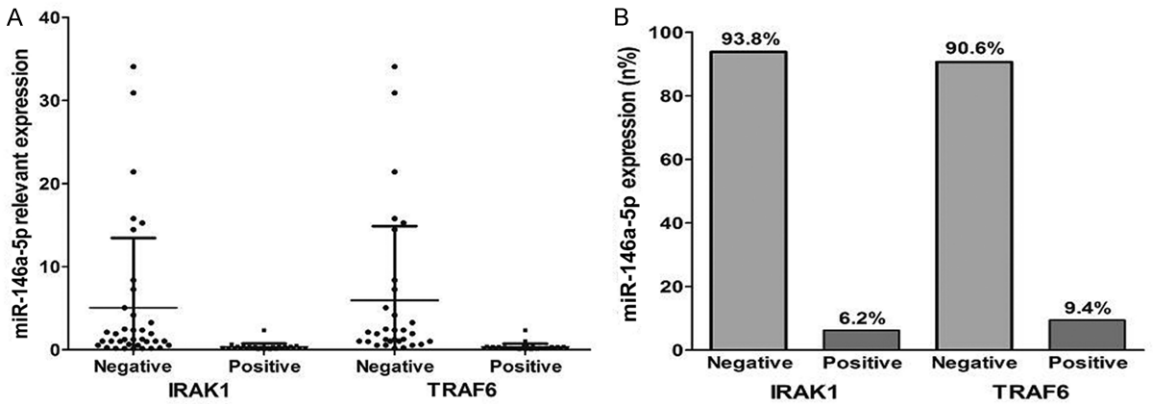

Figure 1. The correlation between miR-146a-5p and IRAK1 or TRAF6. A. The miR-146a-5p relevant expression was negatively correlated with IRAK1 (r=-0.732, P<0.001) and TRAF6 (r=-0.846, P<0.001). Furthermore, the expression of IRAK was positively associated with TRAF6 (r=0.831, P<0.001). B. The miR-146a-5p expression (n%) was negatively correlated with IRAK1 and TRAF6.

Table 3. Detection of the effect of miR-146a-5p, IRAK1 and TRAF6 on proliferation of A549 cells by using MTS assay

Time	0 day			5 days			10 days		
	Mean ± SD	t	*P*	Mean ± SD	t	*P*	Mean ± SD	t	*P*
Blank control	99.67±0.577			100.67±1.155			99.00±1.732		
Negative inhibitor control	100.33±1.155	-0.894	0.422	99.67±0.577	1.342	0.251	100.67±2.082	-1.066	0.346
MiR-146a-5p inhibitor	100.00±1.000	0.378	0.725	103.33±1.155	-4.919	0.008	111.67±2.517	-5.834	0.004
Negative mimic control	100.67±2.082			100.67±1.155			100.33±1.528		
MiR-146a-5p mimic	99.33±0.577	1.069	0.345	96.00±5.196	1.519	0.204	82.33±3.512	8.141	0.001
Negative siRNA control	100.67±2.082			99.00±1.000			100.00±3.464		
IRAK1 siRNA	100.33±0.577	0.267	0.802	90.67±5.132	2.761	0.051	82.33±2.309	7.350	0.002
TRAF6 siRNA	101.67±1.155	-0.728	0.507	82.33±5.508	5.157	0.007	67.33±4.509	9.950	0.001
EGFR siRNA	101.33±1.528	-0.447	0.678	78.00±4.000	8.822	0.001	67.33±3.786	11.026	<0.001

t value was obtained as compared to negative control at same time.

observed with a fluorescence microscope. The apoptosis and morphology of cells could be identified according to the nuclear fragmentation and condensation of chromatin. The number of Hoechst 33342 positive/PI negative viable cells; early apoptotic cells with blue fragmentations; late apoptotic cells with red fragmentations; PI positive necrotic cells and debris signals could be identified [43, 55-57]. The viable, apoptotic, and necrotic cells were counted in at least 10 independent fields under the 200 × vision by two independent persons, and then the average result was compared with the mock control.

Western blot analysis

In this study, Western blot was applied to detect EGFR, IRAK1 and TRAF6 protein expression in NSCLC cells. Firstly, the cells were washed with PBS in a 6-well plate and lysed in a buffer which contains 5 mM EDTA (ph 8), 5% 2-mercaptoeth-

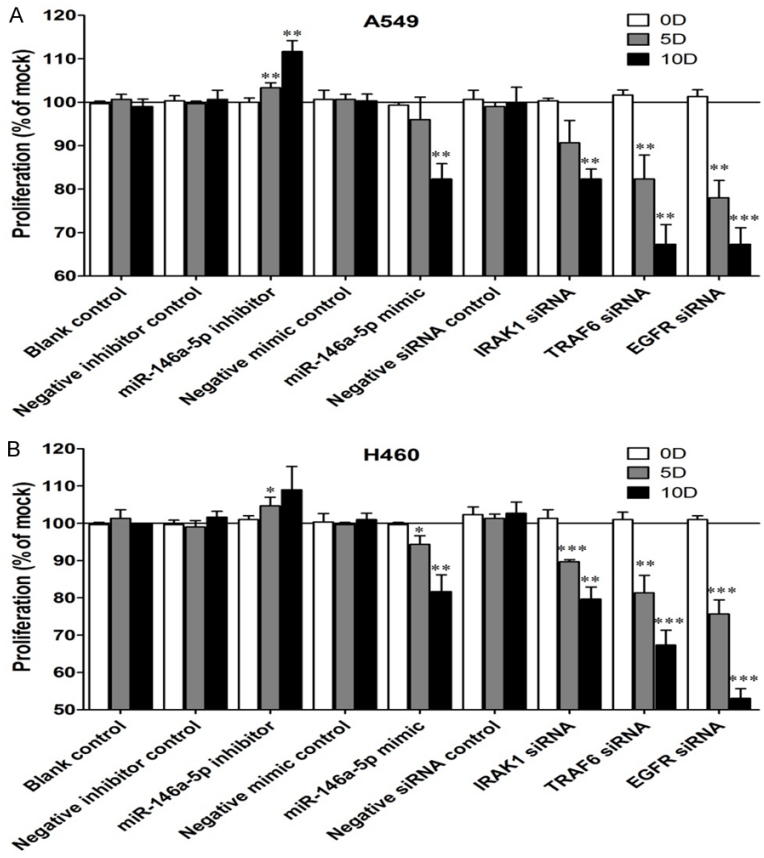

Figure 2. Detection of the effect of miR-146a-5p, IRAK1 and TRAF6 on proliferation of NSCLC cells by using MTS assay. The NSCLC cells were transfected with negative inhibitors, miR-146a-5p inhibitors, negative mimic, miR-146a-5p mimic, negative siRNA, IRAK1 siRNA, TRAF6 siRNA and EGFR siRNA, respectively. A. A549 lung cancer cells; B. H460 lung cancer cells (*P<0.05, **P<0.01).

anol, 5% SDS, 10% glycerol, 0.2% bromophenol blue, 80 mM Tris-HCl (ph 6.8) and 1 mM phenylmethylsulfonyl fluoride. Then, the lysates were centrifuged at 12,000 × g at 4°C for 10 min and boiled for 5 min. Hybond ECL nitrocellulose membranes (GE Healthcare Bio-sciences) were utilized to separate the proteins at 100 mA for 2 h [43, 54, 55, 57, 58]. The membrane was incubated with EGFR (RMA-0554, Santa Cruz Biotechnology, Inc. USA), IRAK1 (sc-5288, Santa Cruz Biotechnology, Inc. USA), TRAF6 (sc-8409, Santa Cruz Biotechnology, Inc. USA) or β-actin (AC-15, Sigma-Aldrich N.V. Bornem, Belgium) antibodies and subjected to chemiluminescence detection assay (GE Healthcare Bio-sciences).

Dual-luciferase reporter assay

The 3'-untranslated region (3'-UTR) of human IRAK1 or TRAF6 was amplified by PCR from the NSCLC cells. And the sequences of miR-146a-5p mimic were: sense, 5' UGAGAACUGAAUUCCAUGGGUU 3' and antisense, 5' CCCAUGGAAUUCAGUUCUCAUU 3'. The sequences of miR-146a-5p negative control were: sense, 5' UCACAACCUCCUAGAAAGAGUAGA 3' and antisense, 5' UACUCUUUCUAGGAGGUUGUGAUU 3'. A partial sequence of the wild-type IRAK1 or TRAF6 3'-UTR containing the miR-146a-5p target site or the IRAK1 or TRAF6 3'-UTR partial sequence lacking the miR-146a-5p target site was templated and cloned into the psiCHECK™-2 vector between the XhoI-PmeI restriction sites in the 3'-UTR of the hRluc gene (Promega, Shanghai, China). The NSCLC cells were co-transfected with luciferase reporter constructs (200 ng) and miR-146a-5p mimic or miR-146a-5p negative control, together with 20 ng pRL-TK vector. The Dual-Luciferase Reporter Assay system was applied for detecting luciferase activities after transfection [55].

Statistical analysis

The expression of miR-146a-5p, IRAK1 and TRAF6 between the two samples was evaluated by Student's t test. The summary statistics were presented as the mean ± standard deviation (Mean ± SD). The relationships between miR-146a-5p expression and IRAK1 and TRAF6 were evaluated by Spearman's rank correlation. A P<0.05 was regarded to be statistically significant (two sides) with SPSS 20.0. In addition, all the experiments were operated with three repetitions.

Results

Correlation between miR-146a-5p and IRAK1 or TRAF6

Among the 65 NSCLC tissue samples, the level of miR-146a-5p was remarkably up-regulated

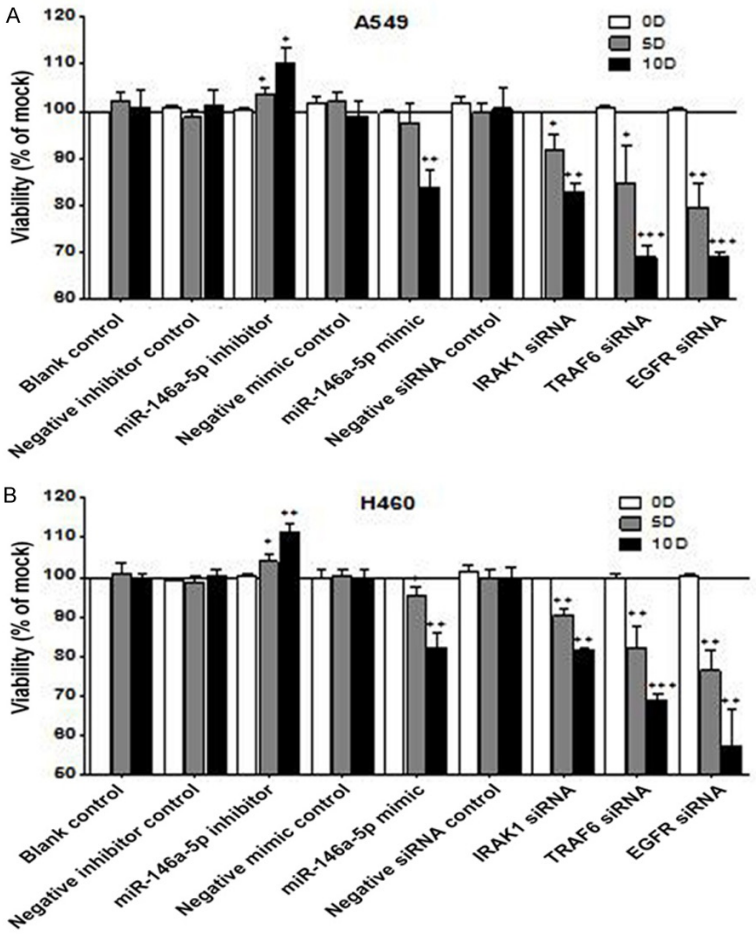

Figure 3. Detection of the effect of miR-146a-5p, IRAK1 and TRAF6 on proliferation of NSCLC cells by using cell viability assay. The NSCLC cells were transfected with negative inhibitors, miR-146a-5p inhibitors, negative mimic, miR-146a-5p mimic, negative siRNA, IRAK1 siRNA, TRAF6 siRNA and EGFR siRNA, respectively. A. A549 lung cancer cells; B. H460 lung cancer cells (*P<0.05, **P<0.01).

in the IRAK1 negative group than in the IRAK1 positive group (5.04273±8.402539 vs. 0.33421±0.422453, P=0.002, **Table 1**). Consistent with IRAK1, the miR-146a-5p expression was higher in the TRAF6 negative group (5.95823±8.908474) than in the TRAF6 positive group (0.33041±0.406994, P=0.001, **Table 1**). Then, to further verify these results, the miR-146a-5p expression was divided into high and low expression group based on the median level of miR-146a-5p. As results, in high miR-146a-5p expression group, the negative rate of IRAK1 expression was 93.8% and the negative rate of TRAF6 expression was 90.6% (both P<0.001, **Table 2**). Similarly, in low miR-146a-5p expression group, the positive rate of IRAK1 expression was 78.8% and the positive rate of TRAF6 expression was 93.9% (both P< 0.001, **Table 2**). Furthermore, to further confirm the correlation between miR-146a-5p and IRAK1 or TRAF6, we performed Spearman's rank correlation test. The results showed that the miR-146a-5p expression was adversely related to IRAK1 (r=-0.732, P<0.001) and TRAF6 (r=-0.846, P<0.001, **Figure 1**). In addition, the IRAK expression was positively associated with TRAF6 in NSCLC (r=0.831, P<0.001, **Figure 1**).

Cell growth effect of miR-146a-5p, IRAK1 and TRAF6 in NSCLC cells

MTS assay, fluorimetric resorufin viability assay and Hoechst 33342/PI double staining assay were performed to evaluate the proliferationof NSCLC cells, respectively. The cell growth effect of A549 and H460 cells at 5 and 10 days after transfection was analyzed. In results of MTS assay, at 5 days after transfection with the miR-146a-5p inhibitor, A549 cell growth was slightly increased in miR-146a-5p inhibitor group than in negative inhibitor control group (103.33±1.155 vs. 99.67±0.577, P=0.008). And cell proliferation was obviously enhanced at 10 days after transfection with miR-146a-5p inhibitor (111.67±2.517 vs. 100.67±2.082, P=0.004, **Table 3**; **Figure 2A**). Consistent with the A549 cell, the cell proliferation in the miR-146a-5p inhibitor group was remarkably enhanced in the H460 cells compared to the negative inhibitor control group (**Figure 2B**). After transfection with miR-146a-5p mimic on the 10th day, a remarkably reduction in growth was noted in both A549 and H460 cells (P<0.01, **Table 3**; **Figure 2**). Similarly, after silencing the expression of IRAK1, TRAF6 or EGFR on the 10th day, the proliferation of A549 and H460 cells was all inhibited than in siRNA control group (P<0.01,

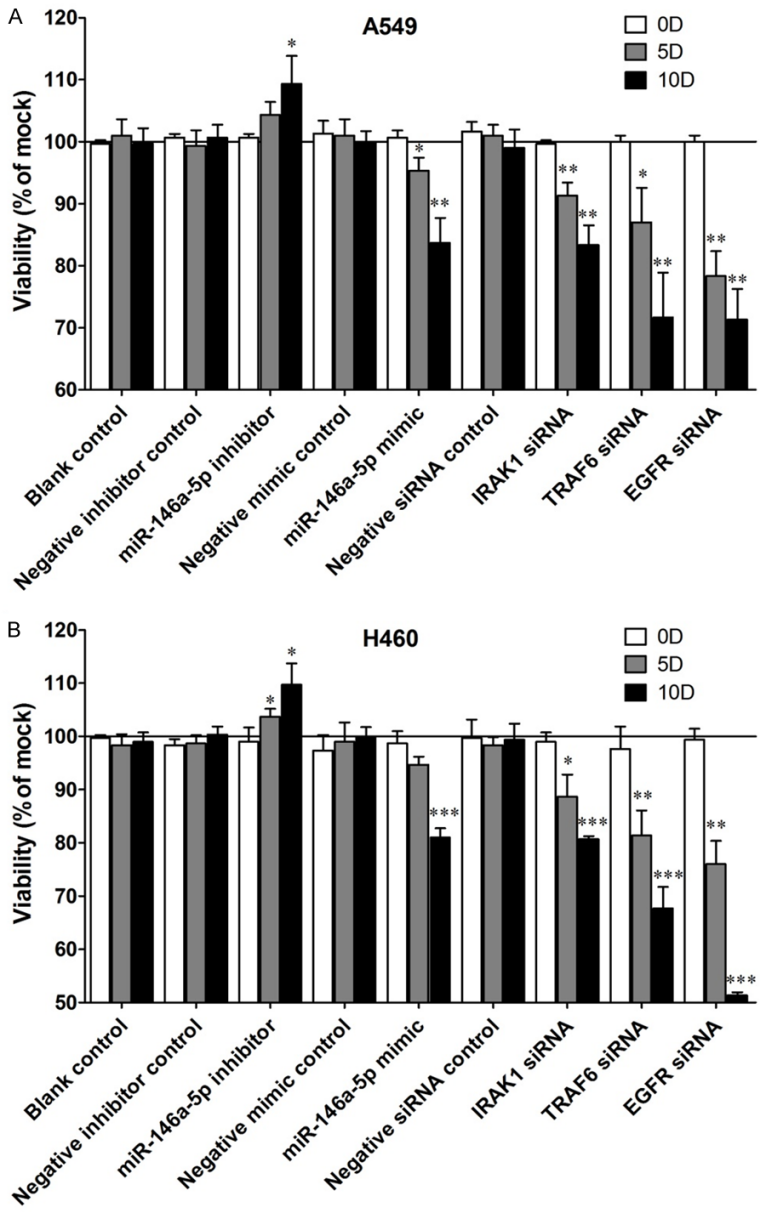

Figure 4. Detection of the effect of miR-146a-5p, IRAK1 and TRAF6 on proliferation of NSCLC cells by using Hoechst 33342 and PI double fluorescent staining assay. The NSCLC cells were transfected with negative inhibitors, miR-146a-5p inhibitors, negative mimic, miR-146a-5p mimic, negative siRNA, IRAK1 siRNA, TRAF6 siRNA and EGFR siRNA, respectively. A. A549 lung cancer cells; B. H460 lung cancer cells (*P<0.05, **P<0.01).

Figure 2). Furthermore, a larger reduction in proliferation was observed in siRNA group than in miR-146a-5p mimic group (**Table 3**; **Figure 2**).

To further confirm these results, a fluorimetric resorufin viability assay was performed to assess the effect on viability. Consistent with MTT assay, we found that a large cell growth promotion was showed in both A549 and H460 cells after transfection with the miR-146a-5p inhibitor. Furthermore, a stronger reduction in proliferation was observed after transfection with miR-146a-5p mimic or siRNA (P<0.05, **Figure 3**).

In addition, Hoechst 33342/PI double staining assay was conducted to microscopic count the viable cells to mirror the effect of miR-146a-5p, IRAK1 and TRAF6 on proliferation. The results showed that the density of viable cells was larger in miR-146a-5p inhibitor group than in negative inhibitor control group (109.33±4.509 vs. 100.67±2.082, P=0.039) on the 10th day in A549 cells. After transfection with miR-146a-5p mimic on the 10th day, the density of viable cells was significantly reduced compared to negative mimic control (83.67±4.041 vs. 100.00±1.732, P=0.003), indicating that miR-146a-5p significantly inhibits the proliferation of A549 cells. After silencing the expression of IRAK1, TRAF6 or EGFR on the 10th day, the cell growth of A549 cells was inhibited than that in siRNA control group (P<0.01, **Figure 4A**). A similar effect on proliferation could be observed in H460 cells (**Figure 4B**).

The results in both assays largely mirrored the effect of miR-146a-5p, IRAK1 and TRAF6 on proliferation. Moreover, these results further verified the reverse relationship between miR-146a-5p and its target genes IRAK1 and TRAF6.

Cell apoptosis effect of miR-146a-5p, IRAK1 and TRAF6 in NSCLC cells

Hoechst 33342 and PI double fluorescent staining assay was utilized to evaluate the

Table 4. Detection of the effect of miR-146a-5p, IRAK1 and TRAF6 on apoptosis of A549 cells by using Hoechst 33342 and PI double fluorescent staining

Time	0 day			5 days			10 days		
	Mean ± SD	t	*p*	Mean ± SD	t	*p*	Mean ± SD	t	*p*
Blank control	1.02±0.035			1.01±0.017			1.00±0.006		
Negative inhibitor control	1.00±0.000	1.000	0.374	1.02±0.040	-0.525	0.627	1.00±0.000	-1.000	0.374
MiR-146a-5p inhibitor	0.99±0.000	/	/	0.99±0.035	0.970	0.387	0.96±0.058	1.300	0.263
Negative mimic control	1.01±0.017			1.02±0.040			1.01±0.017		
MiR-146a-5p mimic	1.04±0.032	-1.265	0.275	1.13±0.121	-1.498	0.208	1.18±0.056	-5.050	0.007
Negative siRNA control	1.01±0.071			1.02±0.035			1.02±0.035		
IRAK1 siRNA	1.04±0.032	-0.519	0.631	1.30±0.081	-5.581	0.005	1.93±0.236	-6.613	0.003
TRAF6 siRNA	1.017±0.038	-0.072	0.946	2.61±0.518	-5.305	0.006	4.72±1.366	-4.695	0.009
EGFR siRNA	1.01±0.0902	0.101	0.925	1.76±0.228	-5.580	0.005	2.26±0.072	-26.849	<0.001

t value was obtained as compared to negative control at same time.

apoptosis affected by miR-146a-5p, IRAK1 and TRAF6 in A549 and H460 cells. The apoptosis rate was 0.96±0.058 folds in A549 cells after transfection with miR-146a-5p inhibitor of 10 days, less than negative inhibitor control group (1.00±0.000, **Table 4**). However, after transfection with the miR-146a-5p inhibitor for 0, 5, 10 days, no statistically significance was observed in NSCLC cells, which indicates that miR-146a-5p inhibitor could induce proliferation, but no obvious change was observed on cell apoptosis. In contrary, after transfection with miR-146a-5p mimics on the 10th day, the apoptosis rate was increased compared to negative mimic control (1.18±0.0557 vs. 1.010±0.017, P=0.007). But no obvious change was observed on 5th day (**Figure 5A**). A similar effect on apoptosis could be observed in H460 cells (**Figure 5B**). Furthermore, after knockdown of IRAK1 and TRAF6, the apoptosis rate was remarkably induced. In A549 cells, TRAF6 siRNA group showed the most obviously effect on apoptosis induction whereas in H460 cells, EGFR siRNA group showed the most potent effect (**Table 4**, **Figure 5**). Besides, the influence on apoptosis was verified microscopically via Hoechst 33342 and PI double fluorescent staining (**Figure 6**).

In addition, the caspase-3/7 assay was used to validate whether miR-146a-5p could induce apoptosis. The results showed that miR-146a-5p inhibitor could not increase caspase-3/7 activity. However, miR-146a-5p mimic could significantly enhance caspase-3/7 activity in A549 cells and H460 cells, but the effect was much less than that in IRAK1 or TRAF6 siRNA group (**Figure 7**).

MiR-146a-5p causes inhibition of IRAK1 and TRAF6 by Western blot in NSCLC cells

To further explore the possible cellular signaling effected by miR-146a-5p, we transfected miR-146a-5p inhibitor and mimic into NSCLC cells. As results, we found that IRAK1, TRAF6 and EGFR were all downregulated after miR-146a-5p mimic transfection similar to IRAK1 siRNA, TRAF6 siRNA and EGFR siRNA in NSCLC cells (data not shown). To confirm the effects of miR-146a-5p on IRAK1 and TRAF6, we transfected miR-146a-5p inhibitor into NSCLC cells and we found that inhibition of miR-146a-5pincreased the levels of IRAK1, TRAF6 and EGFR (data not shown). These results indicated that miR-146a-5p play effects in NSCLC via regulating IRAK1 and TRAF6 signaling.

IRAK1 and TRAF6 are identified as direct targets of miR-146a-5p in NSCLC cells

MIRDB (available online: http://www.mirdb.org/) and Targetscan (available online: http://www.targetscan.org/) were applied to find the potential targets of miR-146a-5p. And IRAK1 and TRAF6 were selected as the candidate genes (**Figure 8**). Then, the dual-luciferase reporter assay was conducted and miR-146a-5p was confirmed to directly bound to the 3'-UTR of IRAK1 and TRAF6 mRNAs (data not shown).

Discussion

Lung cancer is a common disease which threatens human health seriously. An increasing number of studies have revealed that abnormal miRNAs expression is related to the develop-

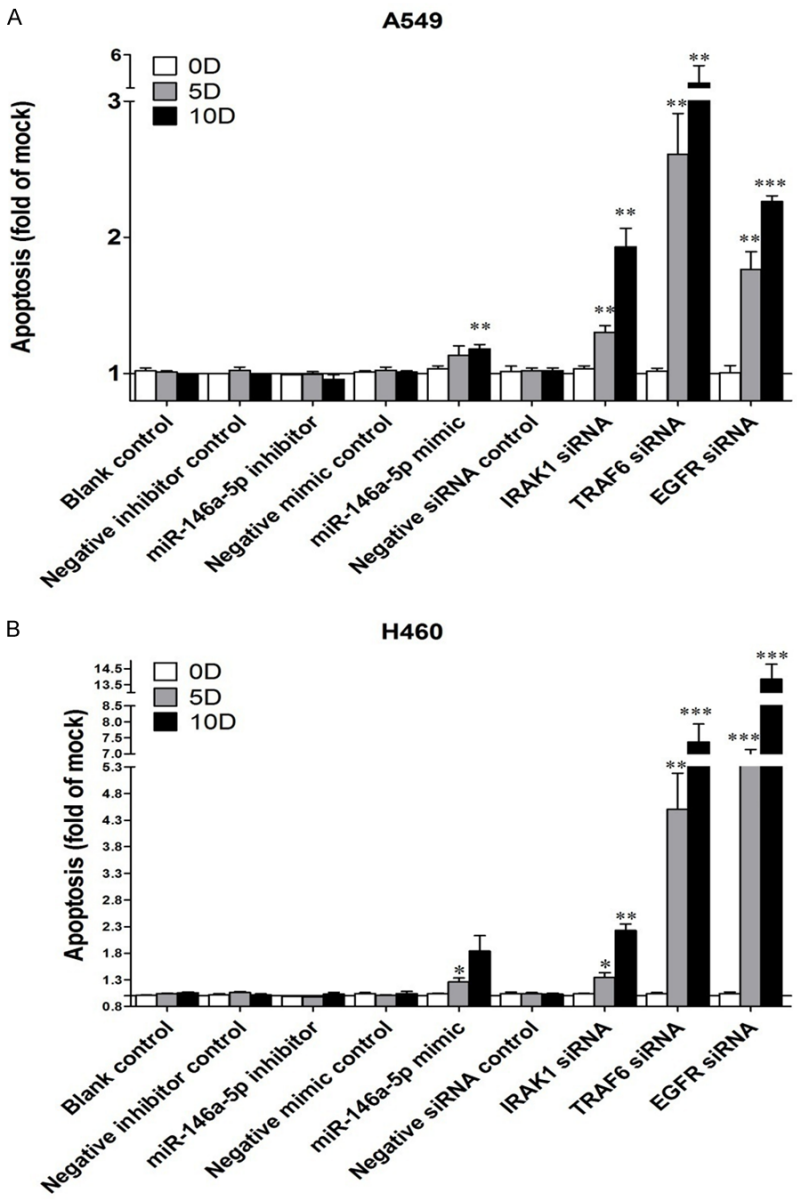

Figure 5. Detection of the effect of miR-146a-5p, IRAK1 and TRAF6 on apoptosis of NSCLC cells by using Hoechst 33342 and PI double fluorescent staining assay. The NSCLC cells were transfected with negative inhibitors, miR-146a-5p inhibitors, negative mimic, miR-146a-5p mimic, negative siRNA, IRAK1 siRNA, TRAF6 siRNA and EGFR siRNA, respectively. A. A549 lung cancer cells; B. H460 lung cancer cells (*P<0.05, **P<0.01).

ment of lung cancer [59, 60]. Zhang [59] et al found that miR-1247 was decreased in NSCLC cells and tumor tissues and miR-1247 overexpression could dramatically inhibit cell proliferation, migration, invasion, and cell cycle progression. Liu [60] et al demonstrated that miRNA-98 plays a suppressive role in NSCLC and the overexpression of miR-98 could suppress the NSCLC proliferation via inhibiting the SALL4 protein expression. Previously, we found that miR-146a-5p was pronouncedly decreased in both NSCLC cells and tumor tissues [25]. And we performed functional experiments *in vitro* to verify that miR-146a-5p could inhibit cell growth and migration and induce cell apoptosis via targeting EGFR and NF-κB signaling. Currently, the EGFR-targeted therapy was applied to clinical therapy gradually, and it might benefit the patients with positive EGFR expression. However, resistance to EGFR-targeted therapies in some lung cancer patients was appeared after treating with EGFR-targeted therapy [61]. Thus, it is imperative to search early diagnostic and novel target for molecular targeted therapy of lung cancer.

IRAK1 and TRAF6 are identified as direct targets of miR-146a-5p by using MIRDB and Targetscan prediction software. In our previous studies, a microarray including 365 lung cancer cases and 30 normal lung cases was constructed to investigate the clinicopathological significance and protein expression of IRAK1 and TRAF6 [52, 53]. The results showed that the IRAK1 and TRAF6 expression were evidently increased in lung cancer compared with that in normal lung tissues. Moreover, the expression of IRAK1 and TRAF6 were positively related to clinical tumor size, TNM stage and lymph node metastasis. In the present study, qRT-PCR and immunohistochemistry were applied to verify the correlation of miR-146a-5p and IRAK1 or TRAF6. Besides, functional experiments *in vitro* were performed to explore the

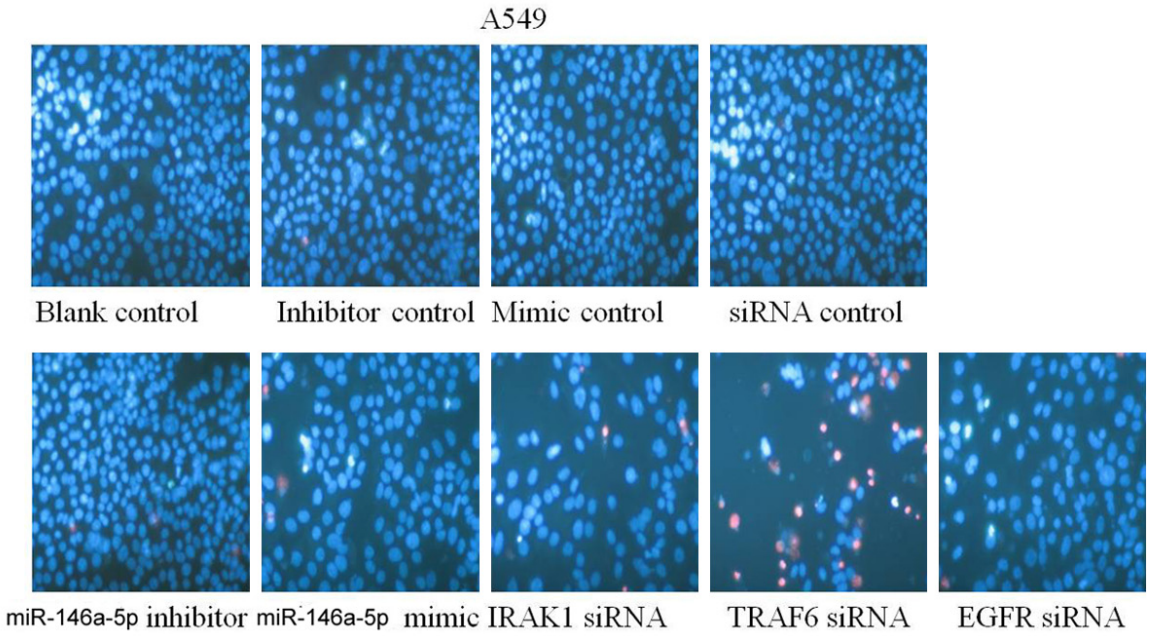

Figure 6. Apoptosis of A549 cells was detected by using Hoechst 33342 and PI double fluorescent staining under microscope. MiR-146a-5p inhibited cell proliferation and inducted apoptosis in NSCLC cells; however, on the contrary, IRAK1 and TRAF6 both promoted lung cancer cells proliferation and inhibited its apoptosis (200 ×).

effect of miR-146a-5p and IRAK1 or TRAF6 on growth and apoptosis at the cellular level. As results, an inverse relationship between miR-146a-5p expression and IRAK1 or TRAF6 was identified. Furthermore, MTS assay, fluorimetric resorufin viability assay and Hoechst 33342/PI double staining assay revealed that the proliferation of NSCLC cells was significantly increased after transfection with miR-146a-5p inhibitor whereas a remarkably reduction in growth was noted after transfection with miR-146a-5p mimic. After silencing the expression of IRAK1 and TRAF6, the proliferation in NSCLC cells was all inhibited which further verified the negatively correlation between miR-146a-5p and IRAK1 or TRAF6. In addition, Hoechst 33342 and PI double fluorescent staining assay and caspase-3/7 activity assay were performed to evaluate the effect of miR-146a-5p and IRAK1 or TRAF6 on cell apoptosis in NSCLC. The results showed that miR-146a-5p mimic could enhance cell apoptosis. And after knockdown of IRAK1 and TRAF6, the cell apoptosis was remarkably induced which further verified our results on the cellular level. To further demonstrate the results of prediction software, a dual-luciferase reporter assay was conducted and the results revealed that miR-146a-5p directly targeted the 3'-UTR of IRAK1 and TRAF6.

Together with the previous study with miR-146a-5p and IRAK1 or TRAF6 on NSCLC, we demonstrated that miR-146a-5p could act as a suppressor in NSCLC and inhibit proliferation and induce apoptosis of NSCLC cells via targeting IRAK1 and TRAF6. The effect of miR-146a-5p and its targets on the growth and apoptosis of NSCLC cells could offer novel evidence on prospective therapeutic targets in the treatment of NSCLC.

Acknowledgements

The study was supported by a Fund the National Natural Science Foundation of China (NSFC81360327, NSFC81560469) and the Natural Science Foundation of Guangxi, China (2015GXNSFCA139009).

Disclosure of conflict of interest

None.

Address correspondence to: Dr. Xiao-Hua Hu, Department of Medical Oncology, First Affiliated Hospital of Guangxi Medical University, 6 Shuangyong Road, Nanning 530021, Guangxi Zhuang Auto-

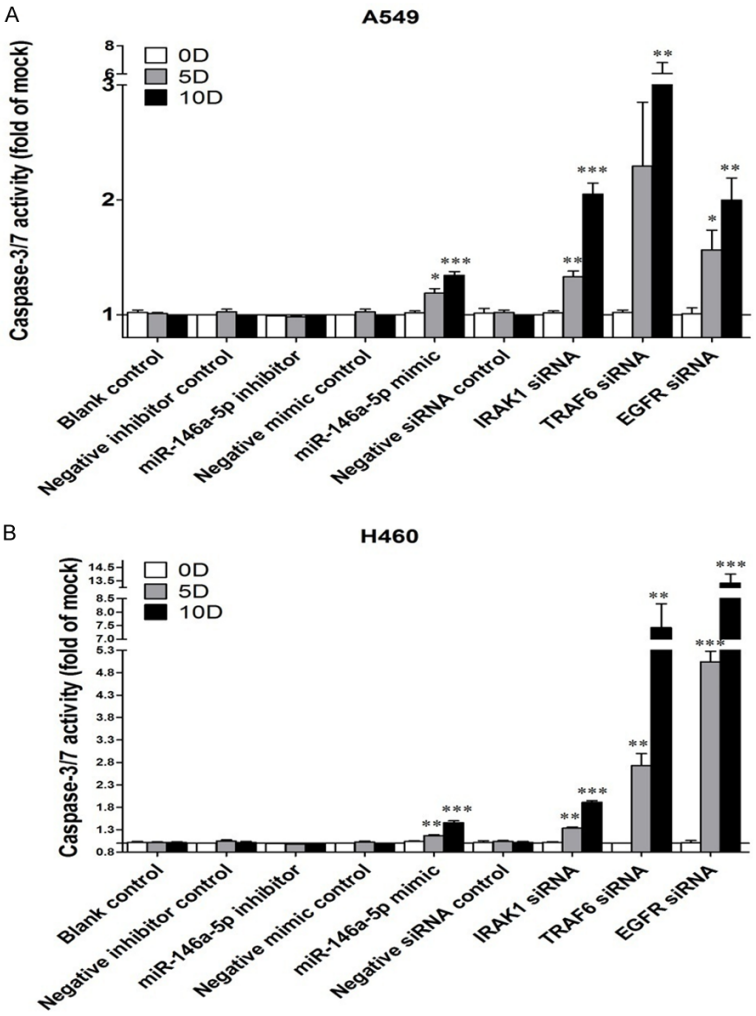

Figure 7. Detection of the effect of miR-146a-5p, IRAK1 and TRAF6 on apoptosis of NSCLC cells by using caspase-3/7 assay. The NSCLC cells were transfected with negative inhibitors, miR-146a-5p inhibitors, negative mimic, miR-146a-5p mimic, negative siRNA, IRAK1 siRNA, TRAF6 siRNA and EGFR siRNA, respectively. A. A549 lung cancer cells; B. H460 lung cancer cells (*P<0.05, **P<0.01).

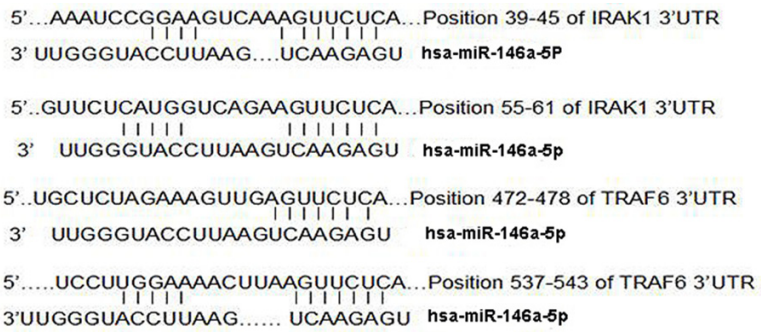

Figure 8. Complementary sequences between miR-146a-5p and IRAK1 or TRAF6.

nomous Region, P. R. China. E-mail: gxmuhxh@163.com; Dr. Gang Chen, Department of Pathology, First Affiliated Hospital of Guangxi Medical University, 6 Shuangyong Road, Nanning 530021, Guangxi Zhuang Autonomous Region, P. R. China. E-mail: chen_gang_triones@163.com

References

[1] Wang FF, Wang S, Xue WH and Cheng JL. microRNA-590 suppresses the tumorigenesis and invasiveness of non-small cell lung cancer cells by targeting ADAM9. Mol Cell Biochem 2016; 423: 29-37.

[2] Peng J, Liu HZ, Zhong J, Deng ZF, Tie CR, Rao Q, Xu W, You T, Li J, Cai CB, Lu Q, Liu W, Zhang Y and Lei ZY. MicroRNA187 is an independent prognostic factor in lung cancer and promotes lung cancer cell invasion via targeting of PTRF. Oncol Rep 2016; 36: 2609-2618.

[3] Bartel DP. MicroRNAs: genomics, biogenesis, mechanism, and function. Cell 2004; 116: 281-297.

[4] Buettner R, Wolf J and Thomas RK. Lessons learned from lung cancer genomics: the emerging concept of individualized diagnostics and treatment. J Clin Oncol 2013; 31: 1858-1865.

[5] Begum S, Hayashi M, Ogawa T, Jabboure FJ, Brait M, Izumchenko E, Tabak S, Ahrendt SA, Westra WH, Koch W, Sidransky D and Hoque MO. An integrated genome-wide approach to discover deregulated microRNAs in non-small cell lung cancer: clinical significance of miR-23b-3p deregulation. Sci Rep 2015; 5: 13236.

[6] Zhang B, Liu T, Wu T, Wang Z, Rao Z and Gao J. MicroRNA-137 functions as a tumor suppressor in human non-small cell lung cancer by targeting SLC22A18. Int J Biol Macromol 2015; 74: 111-118.
[7] Ai C, Jiang R, Fu L and Chen Y. MicroRNA-495 mimics delivery inhibits lung tumor progression. Tumour Biol 2015; 36: 729-735.
[8] Shi WY, Liu KD, Xu SG, Zhang JT, Yu LL, Xu KQ and Zhang TF. Gene expression analysis of lung cancer. Eur Rev Med Pharmacol Sci 2014; 18: 217-228.
[9] Liang J, Zhang Y, Jiang G, Liu Z, Xiang W, Chen X, Chen Z and Zhao J. MiR-138 induces renal carcinoma cell senescence by targeting EZH2 and is downregulated in human clear cell renal cell carcinoma. Oncol Res 2013; 21: 83-91.
[10] Allemani C, Weir HK, Carreira H, Harewood R, Spika D, Wang XS, Bannon F, Ahn JV, Johnson CJ, Bonaventure A, Marcos-Gragera R, Stiller C, Azevedo e Silva G, Chen WQ, Ogunbiyi OJ, Rachet B, Soeberg MJ, You H, Matsuda T, Bielska-Lasota M, Storm H, Tucker TC, Coleman MP and Group CW. Global surveillance of cancer survival 1995-2009: analysis of individual data for 25,676,887 patients from 279 population-based registries in 67 countries (CONCORD-2). Lancet 2015; 385: 977-1010.
[11] Peng Y, Chen FF, Ge J, Zhu JY, Shi XE, Li X, Yu TY, Chu GY and Yang GS. miR-429 inhibits differentiation and promotes proliferation in porcine preadipocytes. Int J Mol Sci 2016; 17.
[12] Zhou Y, Peng Y, Liu M and Jiang Y. MicroRNA-181b inhibits cellular proliferation and invasion of glioma cells via targeting Sal-like protein 4. Oncol Res 2016.
[13] Xu Z, Huang C and Hao D. MicroRNA-1271 inhibits proliferation and promotes apoptosis of multiple myeloma cells through inhibiting smoothened-mediated hedgehog signaling pathway. Oncol Rep 2017; 37: 1261-1269.
[14] Li Z, Lei H, Luo M, Wang Y, Dong L, Ma Y, Liu C, Song W, Wang F, Zhang J, Shen J and Yu J. DNA methylation downregulated mir-10b acts as a tumor suppressor in gastric cancer. Gastric Cancer 2015; 18: 43-54.
[15] Zhang J, Xu L, Yang Z, Lu H, Hu D, Li W, Zhang Z, Liu B and Ma S. MicroRNA-10b indicates a poor prognosis of non-small cell lung cancer and targets E-cadherin. Clin Transl Oncol 2015; 17: 209-214.
[16] Ohdaira H, Sekiguchi M, Miyata K and Yoshida K. MicroRNA-494 suppresses cell proliferation and induces senescence in A549 lung cancer cells. Cell Prolif 2012; 45: 32-38.
[17] Filipowicz W, Bhattacharyya SN and Sonenberg N. Mechanisms of post-transcriptional regulation by microRNAs: are the answers in sight? Nat Rev Genet 2008; 9: 102-114.
[18] Zhen Y, Liu J, Huang Y, Wang Y, Li W and Wu J. MiR-133b inhibits cell growth, migration, and invasion by targeting MMP9 in non-small cell lung cancer. Oncol Res 2016.
[19] Bi M, Chen W, Yu H, Wang J, Ding F, Tang DJ and Tang C. miR-543 is up-regulated in gefitinib-resistant non-small cell lung cancer and promotes cell proliferation and invasion via phosphatase and tensin homolog. Biochem Biophys Res Commun 2016; 480: 369-374.
[20] Ju J, Song B and Wang Y. Impacts of microRNA-215 on cell proliferation and chemotherapy resistance in colon cancer and osteosarcoma. J Clin Oncol 2009; 27: 2542.
[21] Li YL, Wang J, Zhang CY, Shen YQ, Wang HM, Ding L, Gu YC, Lou JT, Zhao XT, Ma ZL and Jin YX. MiR-146a-5p inhibits cell proliferation and cell cycle progression in NSCLC cell lines by targeting CCND1 and CCND2. Oncotarget 2016; 7: 59287-59298.
[22] Wang C, Zhang W, Zhang L, Chen X, Liu F, Zhang J, Guan S, Sun Y, Chen P, Wang D, Un Nesa E, Cheng Y and Yousef GM. MiR-146a-5p mediates epithelial-mesenchymal transition of oesophageal squamous cell carcinoma via targeting Notch2. Br J Cancer 2016; 115: 1548-1554.
[23] Sasaki H, Yoshiike M, Nozawa S, Usuba W, Katsuoka Y, Aida K, Kitajima K, Kudo H, Hoshikawa M, Yoshioka Y, Kosaka N, Ochiya T and Chikaraishi T. Expression level of urinary microRNA-146a-5p is increased in patients with bladder cancer and decreased in those after transurethral resection. Clin Genitourin Cancer 2016; 14: e493-e499.
[24] Cui Y, She K, Tian D, Zhang P and Xin X. MiR-146a inhibits proliferation and enhances chemosensitivity in epithelial ovarian cancer via reduction of SOD2. Oncol Res 2016; 23: 275-282.
[25] Chen G, Umelo IA, Lv S, Teugels E, Fostier K, Kronenberger P, Dewaele A, Sadones J, Geers C and De Greve J. MiR-146a inhibits cell growth, cell migration and induces apoptosis in non-small cell lung cancer cells. PLoS One 2013; 8: e60317.
[26] Forloni M, Dogra SK, Dong Y, Conte D Jr, Ou J, Zhu LJ, Deng A, Mahalingam M, Green MR and Wajapeyee N. MiR-146a promotes the initiation and progression of melanoma by activating Notch signaling. Elife 2014; 3: e01460.
[27] Pacifico F, Crescenzi E, Mellone S, Iannetti A, Porrino N, Liguoro D, Moscato F, Grieco M, Formisano S and Leonardi A. Nuclear factor-{kappa}B contributes to anaplastic thyroid carcinomas through up-regulation of miR-146a. J Clin Endocrinol Metab 2010; 95: 1421-1430.
[28] Zu Y, Yang Y, Zhu J, Bo X, Hou S, Zhang B, Qiu J and Zheng J. MiR-146a suppresses hepatocel-

lular carcinoma by downregulating TRAF6. Am J Cancer Res 2016; 6: 2502-2513.
[29] Hajivalili M, Pourgholi F, Majidi J, Aghebati-Maleki L, Movassaghpour AA, Samadi Kafil H, Mirshafiey A and Yousefi M. G2013 modulates TLR4 signaling pathway in IRAK-1 and TARF-6 dependent and miR-146a independent manner. Cell Mol Biol (Noisy-le-grand) 2016; 62: 1-5.
[30] Gao M, Wang X, Zhang X, Ha T, Ma H, Liu L, Kalbfleisch JH, Gao X, Kao RL, Williams DL and Li C. Attenuation of cardiac dysfunction in polymicrobial sepsis by microRNA-146a is mediated via targeting of IRAK1 and TRAF6 expression. J Immunol 2015; 195: 672-682.
[31] Hung PS, Liu CJ, Chou CS, Kao SY, Yang CC, Chang KW, Chiu TH and Lin SC. miR-146a enhances the oncogenicity of oral carcinoma by concomitant targeting of the IRAK1, TRAF6 and NUMB genes. PLoS One 2013; 8: e79926.
[32] Zhu J and Mohan C. Toll-like receptor signaling pathways--therapeutic opportunities. Mediators Inflamm 2010; 2010: 781235.
[33] Bafica A, Scanga CA, Schito M, Chaussabel D and Sher A. Influence of coinfecting pathogens on HIV expression: evidence for a role of toll-like receptors. J Immunol 2004; 172: 7229-7234.
[34] Baenziger S, Heikenwalder M, Johansen P, Schlaepfer E, Hofer U, Miller RC, Diemand S, Honda K, Kundig TM, Aguzzi A and Speck RF. Triggering TLR7 in mice induces immune activation and lymphoid system disruption, resembling HIV-mediated pathology. Blood 2009; 113: 377-388.
[35] Liu G, Park YJ and Abraham E. Interleukin-1 receptor-associated kinase (IRAK) -1-mediated NF-kappaB activation requires cytosolic and nuclear activity. FASEB J 2008; 22: 2285-2296.
[36] Kobayashi T, Walsh PT, Walsh MC, Speirs KM, Chiffoleau E, King CG, Hancock WW, Caamano JH, Hunter CA, Scott P, Turka LA and Choi Y. TRAF6 is a critical factor for dendritic cell maturation and development. Immunity 2003; 19: 353-363.
[37] Starczynowski DT, Lockwood WW, Delehouzee S, Chari R, Wegrzyn J, Fuller M, Tsao MS, Lam S, Gazdar AF, Lam WL and Karsan A. TRAF6 is an amplified oncogene bridging the RAS and NF-kappaB pathways in human lung cancer. J Clin Invest 2011; 121: 4095-4105.
[38] Zhong L, Cao F and You Q. Effect of TRAF6 on the biological behavior of human lung adenocarcinoma cell. Tumour Biol 2013; 34: 231-239.
[39] Kato S, Yokoyama S, Hayakawa Y, Li L, Iwakami Y, Sakurai H and Saiki I. P38 pathway as a key downstream signal of connective tissue growth factor to regulate metastatic potential in non-small-cell lung cancer. Cancer Sci 2016; 107: 1416-1421.
[40] Mendes VI, Bartholomeusz GA, Ayres M, Gandhi V and Salvador JA. Synthesis and cytotoxic activity of novel A-ring cleaved ursolic acid derivatives in human non-small cell lung cancer cells. Eur J Med Chem 2016; 123: 317-331.
[41] Li Y, Vandenboom TG 2nd, Wang Z, Kong D, Ali S, Philip PA and Sarkar FH. miR-146a suppresses invasion of pancreatic cancer cells. Cancer Res 2010; 70: 1486-1495.
[42] Chen WJ, Gan TQ, Qin H, Huang SN, Yang LH, Fang YY, Li ZY, Pan LJ and Chen G. Implication of downregulation and prospective pathway signaling of microRNA-375 in lung squamous cell carcinoma. Pathol Res Pract 2017; 213: 364-372.
[43] Chen G, Kronenberger P, Teugels E, Umelo IA and De Greve J. Targeting the epidermal growth factor receptor in non-small cell lung cancer cells: the effect of combining RNA interference with tyrosine kinase inhibitors or cetuximab. BMC Med 2012; 10: 28.
[44] Chen G, Kronenberger P, Teugels E and De Greve J. Influence of RT-qPCR primer position on EGFR interference efficacy in lung cancer cells. Biol Proced Online 2010; 13: 1.
[45] Tang R, Liang L, Luo D, Feng Z, Huang Q, He R, Gan T, Yang L and Chen G. Downregulation of miR-30a is associated with poor prognosis in lung cancer. Med Sci Monit 2015; 21: 2514-2520.
[46] Ren F, Ding H, Huang S, Wang H, Wu M, Luo D, Dang Y, Yang L and Chen G. Expression and clinicopathological significance of miR-193a-3p and its potential target astrocyte elevated gene-1 in non-small lung cancer tissues. Cancer Cell Int 2015; 15: 80.
[47] Lan D, Zhang X, He R, Tang R, Li P, He Q and Chen G. MiR-133a is downregulated in non-small cell lung cancer: a study of clinical significance. Eur J Med Res 2015; 20: 50.
[48] Gan TQ, Xie ZC, Tang RX, Zhang TT, Li DY, Li ZY and Chen G. Clinical value of miR-145-5p in NSCLC and potential molecular mechanism exploration: a retrospective study based on GEO, qRT-PCR, and TCGA data. Tumour Biol 2017; 39: 1010428317691683.
[49] Zhang X, Li P, Rong M, He R, Hou X, Xie Y and Chen G. MicroRNA-141 is a biomarker for progression of squamous cell carcinoma and adenocarcinoma of the lung: clinical analysis of 125 patients. Tohoku J Exp Med 2015; 235: 161-169.
[50] Dai J, Wu H, Zhang Y, Gao K, Hu G, Guo Y, Lin C and Li X. Negative feedback between TAp63 and mir-133b mediates colorectal cancer suppression. Oncotarget 2016; 7: 87147-87160.

[51] Wu H, Zhou J, Zeng C, Wu D, Mu Z, Chen B, Xie Y, Ye Y and Liu J. Curcumin increases exosomal TCF21 thus suppressing exosome-induced lung cancer. Oncotarget 2016; 7: 87081-87090.
[52] Zhang XL, Dang YW, Li P, Rong MH, Hou XX, Luo DZ and Chen G. Expression of tumor necrosis factor receptor-associated factor 6 in lung cancer tissues. Asian Pac J Cancer Prev 2014; 15: 10591-10596.
[53] Zhang X, Dang Y, Li P, Rong M and Chen G. Expression of IRAK1 in lung cancer tissues and its clinicopathological significance: a microarray study. Int J Clin Exp Pathol 2014; 7: 8096-8104.
[54] Zhang Y, Huang S, Leng Y, Chen X, Liu T, Wang H, Wei F, Luo D, Chen G and Wei Z. Effect of DcR3-specific siRNA on cell growth suppression and apoptosis induction in glioma cells via affecting ERK and AKT. Onco Targets Ther 2016; 9: 5195-5202.
[55] He R, Yang L, Lin X, Chen X, Lin X, Wei F, Liang X, Luo Y, Wu Y, Gan T, Dang Y and Chen G. MiR-30a-5p suppresses cell growth and enhances apoptosis of hepatocellular carcinoma cells via targeting AEG-1. Int J Clin Exp Pathol 2015; 8: 15632-15641.
[56] Li J, Liang L, Liu Y, Luo Y, Liang X, Luo D, Feng Z, Dang Y, Yang L and Chen G. Clinicopathological significance of STAT4 in hepatocellular carcinoma and its effect on cell growth and apoptosis. Onco Targets Ther 2016; 9: 1721-1734.
[57] Li JJ, Luo J, Lu JN, Liang XN, Luo YH, Liu YR, Yang J, Ding H, Qin GH, Yang LH, Dang YW, Yang H and Chen G. Relationship between TRAF6 and deterioration of HCC: an immunohistochemical and in vitro study. Cancer Cell Int 2016; 16: 76.
[58] Zhang Y, Li ZY, Hou XX, Wang X, Luo YH, Ying YP and Chen G. Clinical significance and effect of AEG-1 on the proliferation, invasion, and migration of NSCLC: a study based on immunohistochemistry, TCGA, bioinformatics, in vitro and in vivo verification. Oncotarget 2017; 8: 16531-16552.
[59] Zhang J, Fu J, Pan Y, Zhang X and Shen L. Silencing of miR-1247 by DNA methylation promoted non-small-cell lung cancer cell invasion and migration by effects of STMN1. Onco Targets Ther 2016; 9: 7297-7307.
[60] Liu W, Xiao P, Wu H, Wang L, Kong D and Yu F. MicroRNA-98 plays a suppressive role in non-small cell lung cancer through inhibition of SALL4 protein expression. Oncol Res 2016.
[61] Egloff AM and Grandis JR. Improving response rates to EGFR-targeted therapies for head and neck squamous cell carcinoma: candidate predictive biomarkers and combination treatment with Src inhibitors. J Oncol 2009; 2009: 896407.